18th Australasian Fluid Mechanics Conference
Launceston, Australia
3-7 December 2012

# Fluid Flow Simulations and Performance Analysis of Turbodrills

**A. Mokaramian[1], V. Rasouli[1] and G. Cavanough[2]**

[1]Deep Exploration Technologies Cooperative Research Centre (DET CRC), and Department of Petroleum Engineering, Curtin University, Perth, WA 6151, Australia.

[2]Deep Exploration Technologies Cooperative Research Centre (DET CRC), and CSIRO, Queensland Centre for Advanced Technologies (QCAT), Brisbane, Q 4069, Australia.

## Abstract

Turbodrill (turbine down hole motor) has been recently proposed by the authors as the preferred drive mechanism with high rotation speed for hard rocks drilling together with impregnated diamond bit for deep mineral exploration applications. The turbine motor section has multistage of rotors and stators which convert the hydraulic power provided by the drilling fluid (pumped from surface) to mechanical power.

This paper presents a methodology for designing turbodrills with asymmetric rotor and stator blades configurations. Also, the results of numerical simulations carried out using computational fluid dynamics (CFD) code for the proposed small size model of turbodrill stage with different drilling fluid types including water, air, and mixture of small water droplets suspended in air (mist) are presented. The results help in performance analysis of this small size turbodrill running with different fluid flow properties to obtain optimum rotational speed and torque during drilling hard rocks for mineral exploration applications.

## Introduction

In mineral exploration, the main purpose of drilling is to acquire large number of samples to obtain information about the vertical and lateral distribution of the ore body. This would determine if the site is feasible for further investigations and studies. With this in mind, drilling small size holes as fast as possible and obtaining the samples to the surface would be a good alternative with several advantages over conventional drilling methods. As a result, the authors have recently proposed Coiled Tube Turbodrilling technology for drilling deep hard rocks mineral exploration [4]. Coiled Tube (CT) is a continuous length of ductile steel or carbon fiber tube that is stored and transported over a large reel. Coiled tube itself cannot rotate and therefore a down hole motor is needed to provide mechanical power to the bit. There are many special design criteria to be considered for successful operation of down hole motors in CT drilling; One major concern is that it is often difficult to produce enough weight on bit (WOB) to maximize the rate of penetration (ROP) for optimised drilling. In an environment where WOB is limited (as with CT drilling); high rotation speed is the key driver for ROP [1]. Amongst the down hole motors, turbodrills (turbine motors) are the best choice to be used for small size CT drilling in hard rocks, providing a smooth borehole with little vibrational effects during drilling with high output rotational speed [3]. Figure 1 shows schematic of a coiled tubing unit with the main assembly proposed for hard rocks mineral exploration drilling.

Turbodrill is a type of hydraulic axial turbomachinery which has multistage of stators and rotors. It converts the hydraulic power provided by the drilling fluid pumped from surface to mechanical power through turbine motor with diverting the fluid flow through the stator vanes to the rotor vanes. The energy required to change the rotational direction of the drilling fluid is transformed into rotational and axial (thrust) force. This energy transfer is seen as a pressure drop in the drilling fluid. The thrust is typically absorbed by the thrust bearings. The rotational force causes the rotor to rotate relative to the housing. In practice, multiple stages are stacked coaxially until the desired power and torque is achieved. The main operating parameters that dictate the size of the turbine motors are torque, speed, and mud flow rate and weight. Due to hydrodynamics, the output power of a turbine motor is not linear with the mud flow rate and 20% decrease in the flow rate causes a 50% reduction in the turbine motor output power [5].

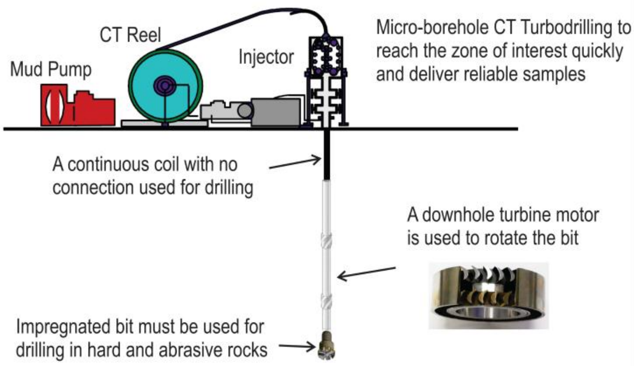


Figure 1. Schematic of a coiled tubing unit with main assembly proposed for hard rocks mineral exploration drilling.

## Turbodrill Design

When designing a hydraulic multistage turbine, it is assumed that each turbine stage is identical (i.e., that the flow rate, pressure drop, rotary speed, generated torque, and power transmitted to the shaft are the same for each of the stages).

The well-known method of building velocity triangles is used when designing the blade unit profile. This method is useful for visualizing changes in the magnitude and direction of the fluid flow due to its interaction with the blade system. The analysis of the flow-field within the rotating blades of a turbodrill is performed in a frame of reference that is stationary relative to the blades. In this frame of reference the flow appears as steady, whereas in the absolute frame of reference it would be unsteady. This makes any calculations significantly more straightforward and therefore relative velocities and relative flow quantities are used in this study.

Three key non-dimensional parameters are related to the shape of the turbine velocity triangles and are used in fixing the preliminary design of a turbine stage, which are described as design flow coefficient, stage loading coefficient, and stage reaction. These are discussed below:

### Design Flow Coefficient

Design flow coefficient is defined as the ratio of the meridional flow velocity to the blade speed, $\emptyset = c_m/U$, [2]. In general, the flow in a turbomachine has components of velocity along all three cylindrical axes (axial $x$, radial $r$, and tangential $r_\theta$ axes). However, for turbodrill, to simplify the analysis it is assumed that the flow does not vary in the tangential direction. In this case, the flow moves through the machine on axi-symmetric stream surfaces. The component of velocity along an axi-symmetric stream surface is called the meridional velocity ($c_m$), expressed as:

$$c_m = \sqrt{c_x^2 + c_r^2} \; . \tag{1}$$

In purely axial-flow machines such as turbodrill, the radius of the flow path is constant and therefore, the radial flow velocity will be zero and $c_m = c_x$. As a result, the flow coefficient for turbodrill is defined as:

$$\phi = \frac{c_x}{U} \; . \tag{2}$$

The value of $\emptyset$ for a stage determines the relative flow angles. A stage with a low value of $\emptyset$ implies highly staggered blades and relative flow angles close to tangential axis, whereas high values imply low stagger and flow angles closer to the axial axis [2].

### Stage Loading

The stage loading is defined as the ratio of the stagnation enthalpy change through a turbine stage to the square of the blade speed, $\psi = \Delta h_0/U^2$ [2]. In turbodrill that is an adiabatic turbine, the stagnation enthalpy change is equal to the specific work, ΔW, and because it is a purely axial turbine with constant radius, we can use the Euler work equation ($\Delta W = U \times \Delta c_\theta$) to write, $\Delta h_0 = U \times \Delta c_\theta$. As a result, the stage loading for turbodrill can be written as:

$$\psi = \frac{\Delta c_\theta}{U} \; . \tag{3}$$

where $\Delta c_\theta$ represents the change in the tangential component of absolute velocity through the rotor. Thus, high stage loading means large flow turning and leads to highly "skewed" velocity triangles to achieve this turning. Since the stage loading is a non-dimensional measure of the work extraction per stage, a high stage loading is desirable because it means fewer stages needed to produce a required work output [2].

### Stage Reaction

The stage reaction is defined as the ratio of the static enthalpy drop in the rotor to the static enthalpy drop across the turbine stage [2]:

$$R = \frac{h_2 - h_3}{h_1 - h_3} \; . \tag{4}$$

Taking the flow through a turbodrill as isentropic, the equation of the second law of thermodynamics, $Tds = dh - dp/\rho$ can be approximated by $dh = dp/\rho$, and ignoring compressibility effects, the reaction can thus be obtained as [18]:

$$R = \frac{p_2 - p_3}{p_1 - p_3} \; . \tag{5}$$

The reaction therefore indicates the drop in pressure across the rotor compared to that of the stage. It describes the asymmetry of the velocity triangles and is therefore a statement of the blade geometries. Typically, in prior turbodrills designs a 50% reaction were selected (i.e. the stator blades and the rotor blades are symmetric). Axial thrust resulting from the reaction on the rotor blade is typically absorbed by thrust bearings. A higher reaction typically increases the thrust created by the rotor vane, which must then be absorbed by thrust bearings. By significantly reducing the amount of axial thrust absorbed by the thrust bearings, the friction in the thrust bearings can be reduced, thereby decreasing resistance to rotation of the shaft and increasing the efficiency of the turbodrill as a whole.

The main goal in the preliminary stage design of a turbine and in this study is to fix the shapes of the velocity triangles, either by setting the flow angles or by choosing values for the three dimensionless design parameters, $\emptyset$, $\psi$, and $R$.

From the specification of the turbodrill, the design will usually have a known mass flow rate of the drilling fluid and a required power output. As a result, the specific work per stage can be determined from the stage loading and the blade speed and, consequently, the required number of stages can be found as following:

$$n_{stage} \geq \frac{\Delta W}{\psi U^2} \; . \tag{6}$$

## Turbodrill Model

The shroud (housing) and hub (shaft) diameters of the turbodrill for the applications of this study were set to be 5 and 2 cm, respectively. Consequently, the spanwise height (H) will be 1.5 cm for this model with 10 blades on each row and there is no shroud tip between blade tip and housing, i.e. the blades are connected to the housing. Figure 2 shows the geometry model of the one stage turbodrill prepared for the simulation which is shown here without housing for better illustration.

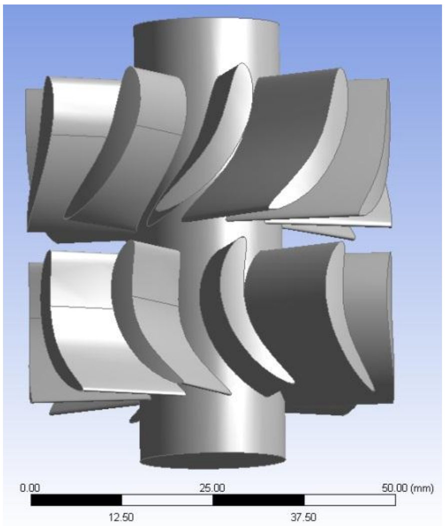


Figure 2. Geometry model of the one stage turbodrill with 10 blades on each row.

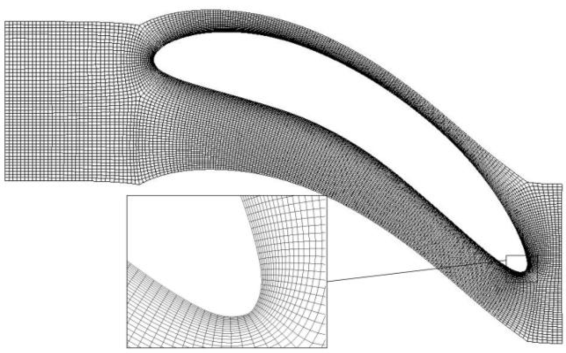

Figure 3. Blade to blade view of the high quality hexahedral mesh for the stator at mid-span.

After building the geometry of blades row on the stator and rotor, a three-dimensional high quality hexahedral mesh with mesh resolution of about $1\times10^6$ numbers of hexahedral elements per each stage was generated to obtain high quality output simulation results. The boundary layer is resolved to ensure a near-wall y+ of less than 1 to comply with wall function constraints. Figure 3 shows the blade to blade view of the high quality mesh for the stator at mid-span.

## Numerical Simulations

In this study with the objective of Turbodrill performance analysis running with different fluid flow properties, CFD simulations using the finite volume technique of various mass flow rates of each fluid type have been analysed. In this paper, only a few of the simulation results for one stage of the proposed turbodrill model are presented for different drilling fluid of water, air, and mixture of water droplets suspended in air (mist), to investigate the turbodrill performance especially the optimum rotation speed under different fluid flow conditions. Water particle was added to provide cooling to the down hole assembly especially the diamond bit which is crushing the rocks by grinding it to very small cuttings in the range of about 100 micron. Also, the use of misting agents reduces the possibility of ignition down hole when drilling with air. Here, the objective is to increase optimized output rotation speed suitable for hard rocks CT Turbodrilling system to reach higher drilling rates.

In this study the flow field is calculated based on the Reynolds-Averaged Navier–Stokes (RANS) equations which are derived from the governing Navier–Stokes equations by decomposing the total relevant flow variables into a mean quantity (time-averaged component) and fluctuation component (i.e. for velocity, $u=U+u'$). Here, time-averaged RANS equations, supplemented with two turbulence models of the k-ε (k-epsilon) for water and shear stress transport (SST) which uses a combination of the k-ε and k-ω (k-omega) for air and mist flow have been used in CFD simulations. Substituting the averaged quantities into the original Navier–Stokes transport equations results in the RANS equations given below in tensor notation:

$$\frac{\partial \rho}{\partial t}+\frac{\partial}{\partial x_j}\left(\rho U_j\right)=0, \tag{7}$$

$$\frac{\partial \rho U_i}{\partial t}+\frac{\partial}{\partial x_j}\left(\rho U_i U_j\right)=-\frac{\partial p}{\partial x_i}+\frac{\partial}{\partial x_j}\left(\tau_{ij}-\rho\overline{u_i u_j}\right)+S_M, \tag{8}$$

where $\tau$ is the stress tensor (including both normal and shear components of the stress) defined as below:

$$\tau_{ij}=\mu\left(\frac{\partial U_i}{\partial x_j}+\frac{\partial U_j}{\partial x_i}\right)-\rho\overline{u_i' u_j'}\,. \tag{9}$$

The Reynolds averaged energy equation in tensor notation is:

$$\frac{\partial \rho h_{tot}}{\partial t}-\frac{\partial p}{\partial t}+\frac{\partial}{\partial x_j}\left(\rho U_j h_{tot}\right)=\frac{\partial}{\partial x_j}\left[\lambda\frac{\partial T}{\partial x_j}-\rho\overline{u_j h}\right]$$
$$+\frac{\partial}{\partial x_j}\left[U_i(\tau_{ij}-\rho\overline{u_i u_j})\right]+S_E\,, \tag{10}$$

where, $h_{tot}$ is the total enthalpy, related to the static enthalpy, $h$, by $h_{tot}=h+0.5\,U^2$.

For an incompressible Newtonian fluid (i.e. for water), the RANS equations are expressed in tensor notation as following:

$$\rho\frac{\partial U_i}{\partial t}+\rho U_j\frac{\partial U_i}{\partial x_j}=\rho\overline{f}_i+\frac{\partial}{\partial x_j}\left[-p\delta_{ij}+2\mu\overline{S}_{ij}-\rho\overline{u_i' u_j'}\right], \tag{11}$$

where $f_i$ is a vector representing external forces and $\delta_{ij}$ is the Kronecker delta function ($\delta_{ij}$=1 if $i=j$ and $\delta_{ij}$=0 if $i\neq j$). Also, $S_{ij}$ is the mean rate of strain tensor:

$$\overline{S}_{ij}=\frac{1}{2}\left(\frac{\partial U_i}{\partial U_j}+\frac{\partial U_j}{\partial x_i}\right) \tag{12}$$

In this study, because of the periodic symmetry between the blades on stator row and also on rotor row and having the same number of blades on each row, i.e. pitch ratio of 1, the simulations were conducted for one blade of stator and one blade of rotor interacting with each other. The results will show velocity vectors and pressure profiles on the meridional view of the flow passage at 50% span.

## Simulation Results

In overall, the simulation results show that the turbodrill performance is highly dependent on the mass flow rate of the drilling fluid. As the mass flow rate is increased the expected optimum rotation speed and output power of the turbodrill increases. While the mass flow rate of the drilling fluid reduces, the output rotation speed, the power and consequently shaft torque will drastically decrease to allow the velocity vectors entering rotor be aligned with the rotor inlet angle (to be effective in producing rotational effects on the rotor blades). Figure 4 and 5 show the CFD simulation results for water and air with 7 Kg/s and 0.1 Kg/s of mass flow rates, respectively. From these result it is clear that with air, it can be possible to have higher rotation speed (10,000 rpm in our case). For water, due to limitations on the mass flow rates that can be injected from the surface pump down through the CT assembly to bottom hole to actuate the turbodrill (having huge pressure losses through the drilling assembly), the practical mass flow rates for this small size CT assembly should be below 7 Kg/s, and here with the mass flow rate of 7 Kg/s it can be reached to 4,000 rpm of optimum rotation speed. With the higher rotation speed, it will result to less power and efficiency.

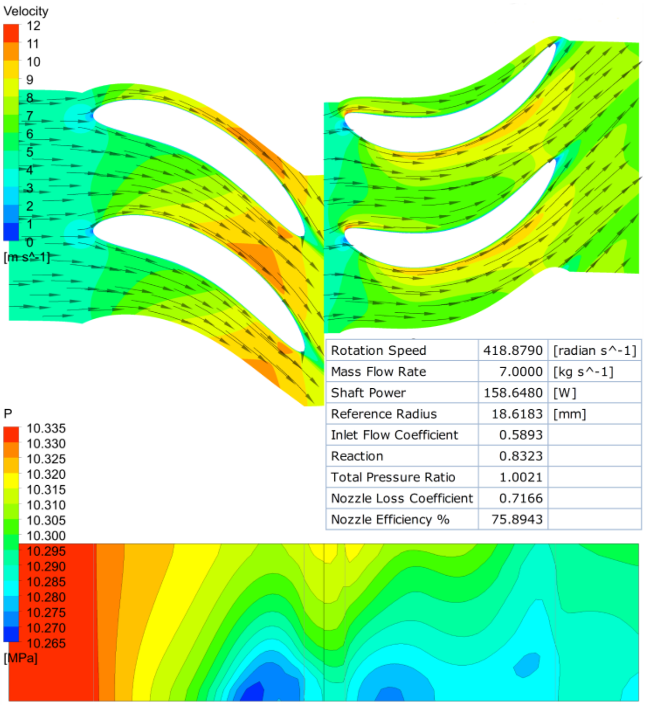


Figure 4. Water flow simulation through small turbodrill model with mass flow rate of 7 Kg/s and rotation speed of 4,000 rpm.

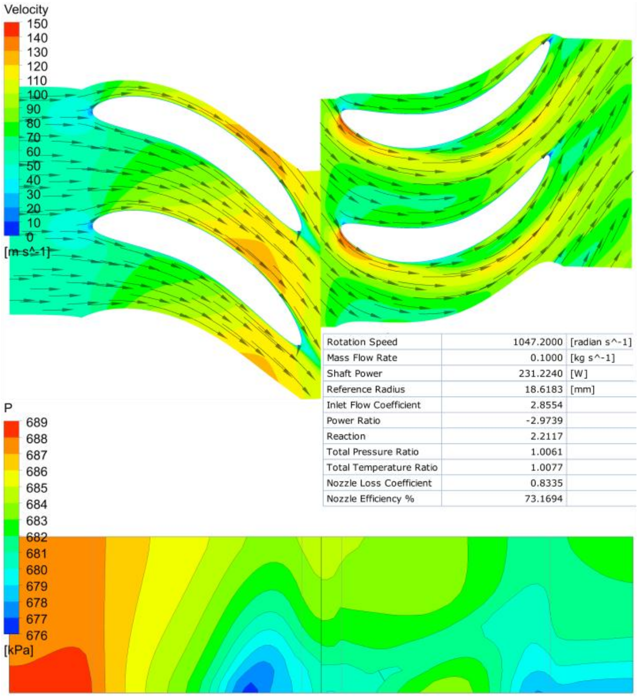


Figure 5. Air flow simulation through small turbodrill model with mass flow rate of 0.1 Kg/s, and rotation speed of 10,000 rpm.

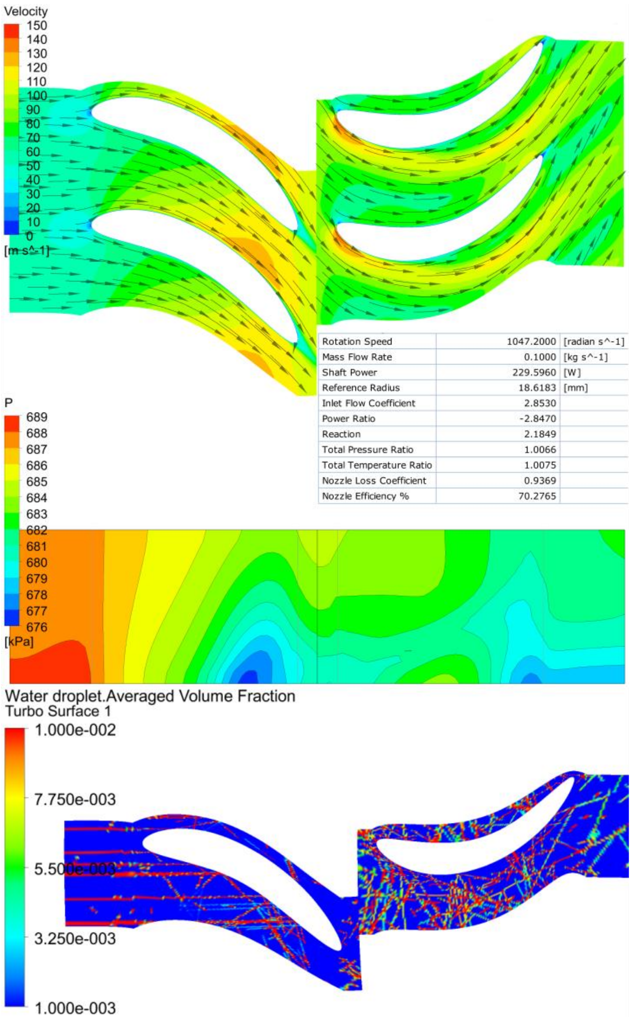


Figure 6. Two phase flow (mist) simulation of air (0.1 Kg/s) as continuous phase and water droplets (0.1 Kg/s) as dispersed fluid particle.

Figure 6 shows the simulation results for the two phase flow (mist) of air as continuous phase and water droplets as dispersed fluid particle. A Lagrangian particle tracking multiphase model with the choice of full coupling with the continuous phase and the Schiller-Naumann drag model together with Ranz-Marshall correlations for heat transfer were used. In this paper only the result of one mist mixture (equal mass flow rate of 0.1 Kg/s for both air and water particle) is presented. In each time step 1000 particles of water with 1 mm specified diameter are injected to the system in the same temperature with air flow (25 °C). This figure also shows the average volume fraction of water particle for 0.1 Kg/s mass flow rate of water injection.

## Conclusions

A design methodology for a small size Turbodrill (turbine down hole motor) optimised for small size Coiled Tube (CT) Turbodrilling system for deep hard rocks mineral exploration applications was presented. The results of numerical simulations for turbodrill stage performance with asymmetric blades profiles on stator and rotor running with different drilling fluid types including water, air, and two phases drilling fluid flow (mist) of air as continuous phase and water droplets as dispersed fluid particle were reported.

The simulation results for the specific proposed blades configuration showed that the turbodrill performance is highly dependent on the mass flow rate of the drilling fluid, i.e. as the mass flow rate increases the expected rotation speed of the turbodrill and consequently the output power and torque will increase. With air and mist it can be possible to have higher output rotation speed and power than with water with their operationally applicable mass flow rates.

## Acknowledgments

The authors would like to express their sincere thanks to the Deep Exploration Technologies Cooperative Research Centre (DET CRC) for their financial supports towards this project. This paper is DET CRC Document 2012/027.

## References

[1] Beaton T., Seale R., The Use of Turbodrills in Coiled Tubing Applications, SPE/ICoTA Coiled Tubing Conference (SPE 89434), Houston, Texas, U.S.A., 2004.

[2] Dixon S. L., Hall C. A. Fluid Mechanics and Thermodynamics of Turbomachinery. Sixth ed. The United States of America, Elsevier Inc., 2010.

[3] Mokaramian A., Rasouli V., Cavanough G., Adapting oil and gas downhole motors for deep mineral exploration drilling, in *Deep Mining 2012: Proceedings of the sixth International Seminar on Deep and High Stress Mining*, editor Potvin Y, Perth, Western Australia, Australian Centre for Geomechanics (ACG); 2012, pp. 475-86.

[4] Mokaramian A., Rasouli V., Cavanough G., A feasibility study on adopting coiled tubing drilling technology for deep hard rock mining exploration, in *Deep Mining 2012: Proceedings of the sixth International Seminar on Deep and High Stress Mining*, editor Potvin Y, Perth, Western Australia, Australian Centre for Geomechanics (ACG); 2012, pp. 487-99.

[5] Reich M., Picksak A., John W., Regener T., Competitive Performance Drilling with High-Speed Downhole Motors in Hard and Abrasive Formations, IADC/SPE Drilling Conference (IADC/SPE 59215), New Orleans, Louisiana, 2000.